ISTITUTO PER LA MATEMATICA APPLICATA
CONSIGLIO NAZIONALE DELLE RICERCHE
Via De Marini, 6
16149 Genova, Italia

TRIANGLE MESH DUALITY: RECONSTRUCTION AND SMOOTHING[1]

G. Patané

Technical Report N$^{\diamond}$. 3/2002

[1]Istituto per la Matematica Applicata, Consiglio Nazionale delle Ricerche, Genova, Italia.
email: patane@ima.ge.cnr.it

1. ABSTRACT

Current scan technologies provide huge data sets which have to be processed considering several application constraints. The different steps required to achieve this purpose use a structured approach where fundamental tasks, e.g. surface reconstruction, multi-resolution simplification, smoothing and editing, interact using both the input mesh geometry and topology. This paper is twofold; firstly, we focus our attention on duality considering basic relationships between a 2-manifold triangle mesh $\mathcal{M}$ and its dual representation $\mathcal{M}'$. The achieved combinatorial properties represent the starting point for the reconstruction algorithm which maps $\mathcal{M}^{'}$ into its primal representation $\mathcal{M}$, thus defining their geometric and topological identification. This correspondence is further analyzed in order to study the influence of the information in $\mathcal{M}$ and $\mathcal{M}^{'}$ for the reconstruction process. The second goal of the paper is the definition of the "*dual Laplacian smoothing*", which combines the application to the dual mesh $\mathcal{M}^{'}$ of well-known smoothing algorithms with an inverse transformation for reconstructing the regularized triangle mesh. The use of $\mathcal{M}^{'}$ instead of $\mathcal{M}$ exploits a topological mask different from the 1-neighborhood one, related to Laplacian-based algorithms, guaranteeing good results and optimizing storage and computational requirements.

2. Introduction

Recent applications to compression [13], smoothing [18], subdivision [21] reveal an increasing attention to the correspondence between a mesh $\mathcal{M}$ and its dual representation $\mathcal{M}^{'}$. The growing interest on primal-dual correspondence is due to a greater regularity of the dual mesh topology which corresponds to storage and computational optimization. The first part of the paper analyzes in detail the topological and geometric identification between $\mathcal{M}$ and $\mathcal{M}^{'}$; more precisely, we provide a reconstruction algorithm of the geometry of $\mathcal{M}$ through that of $\mathcal{M}^{'}$, also achieving basic combinatorial properties of the 1-neighborhood of each internal vertex in $\mathcal{M}$. This correspondence results in the definition of a discrete homeomorphism between $\mathcal{M}$ and $\mathcal{M}^{'}$ whose computational cost is linear in the number of faces in $\mathcal{M}$. The stability to noise on the mesh vertices is studied underlining the correlation between adjacent neighborhoods in $\mathcal{M}$. The developed framework is used to look at the signal processing theory of triangle meshes by considering the dual mesh as noised one, and successively defining the regularized mesh through a process different from the primal-dual identification which cannot be applied due to the violation of the derived combinatorial properties. Therefore, the "*dual Laplacian smoothing*" reveals the way the regularization process affects the input mesh geometry. This approach to smoothing enables to consider a new topological mask for the mesh regularization whose effectiveness is compared with that of the Taubin's $\lambda|\mu$ algorithm [17].

The paper is organized as follows: in Section 3 definitions and properties of 3D polygonal meshes and duality are given. Combinatorial relations and triangle mesh reconstruction through duality are discussed in Section 4, providing several considerations on the primal-dual correspondence. The dual Laplacian smoothing is analyzed in Section 5 underlining its relationship with analogous methods and triangle mesh duality previously analyzed. Conclusions and future work are discussed in the last section.

3. Polygonal meshes and duality

A *polygonal mesh* is defined by a pair $\mathcal{M} := (P, F)$ where P is a set of vertices $P := \{p_i := (x_i, y_i, z_i) \in \mathbb{R}^3,\ i = 1, \ldots, n_V\}$, and F an abstract simplicial complex which contains the connectivity information, i.e. the mesh topology. In particular, if we consider a *triangle* *mesh* each element in the complex F comes into one of these elements: vertex $\{i\}$, edge $\{i,j\}$, face $\{i,j,k\}$. Traversing the mesh is achieved by using the relations [14]:

- vertex-vertex $VV(v) = (v_1, \dots, v_k)$, face-face $FF(f) = (\tilde{f}_1, \dots, \tilde{f}_m)$;
- face-vertex $VF(v) = (f_1, \dots, f_k)$, vertex-face $FV(f) = (v_1, \dots, v_q)$.

In the following of the paper we assume that the previous relations are consistently evaluated. A vertex v is defined as *internal* if its *1-neighborhood* $VV(v)$ is closed, i.e. v is not on the boundary of $\mathcal{M}$. Different authors have proposed optimized data structures [10, 14] for efficiently representing and traversing a polygonal mesh; specializations of these techniques to triangle meshes are described in [6]. The duality of structures arises in different scientific contexts such as functional/numerical analysis (e.g. dual of Hilbert spaces) and computational geometry. In the last field one of the fundamental data structure is the Voronoi diagram [1, 5, 8, 10, 16] of a discrete set of points. Its study, which has influenced different application areas such as math, computer and natural science, is strictly related to the Delaunay triangulation and their duality relationships. In the sequel of the section we briefly review the duality in the plane and its extension to 3D meshes. If $P := \{p_i\}_{i=1}^{n_V}$ is a set of n_V points in $\mathbb{R}^d$, its *Voronoi diagram* $V(P)$ is a cell complex which decomposes $\mathbb{R}^d$ into n_V cells $\{V(p_i)\}_{i=1}^{n_V}$ where $V(p_i)$ is defined as

$$V(p_i) := \{x \in \mathbb{R}^d : \|x - p_i\|_2 < \|x - p_j\|_2, j \neq i\}$$

and $\| \, \|_2$ denotes the Euclidean distance. This definition introduces a proximity relation among points in $\mathbb{R}^d$. In the planar case, i.e. $d = 2$, the *dual graph* $\mathcal{G}$ of $V(p)$ has a node for every cell and it has an arc between two nodes if the corresponding cells share an edge. The *Delaunay graph* of P is defined as the straight-line embedding of $\mathcal{G}$ obtained by identifying the node corresponding to the cell $V(p_i)$ with p_i and the arc connecting the nodes of $V(p_i)$ and $V(p_j)$ with the segment $\overline{p_i p_j}$. The Delaunay graph of a planar point set is a plane graph and, if P is in *general position*, i.e. no four points lie on a circle, all vertices of the Voronoi diagram have degree three. This result guarantees that all bounded faces in the Delaunay graph are triangles, thus defining the *Delaunay triangulation* of P. The extension of this theory for triangulating a set of points in $\mathbb{R}^3$ is not trivial; as a result important properties of the two dimensional Delaunay triangulation, e.g. optimal storage requirement, computational cost, partially apply to the 3D setting. Previous considerations have required the definition of new algorithms [3, 11], and 3D triangulation remains a challenging problem in Computer Graphics. From a geometric point of view, this has also brought a diminishing attention to duality mainly due to the use of other geometric structures.

The use of several algorithms for constructing a polygonal mesh of a 3D point cloud requires to define the dual graph in a general way, taking out of consideration the method that has been used for the mesh construction. Given a polygonal mesh $\mathcal{M}$, its *dual graph* $\mathcal{G}$ has a node $v^\star$ for each face $f(v^\star)$ in $\mathcal{M}$ and it has an arc between two nodes $v^\star$ and $w^\star$ if and only if $f(v^\star)$ and $f(w^\star)$ share an edge (see Figure 1). In analogy with the previous definitions, the *barycenter dual graph* of $\mathcal{M}$ is defined as the straight-line embedding $\mathcal{M}'$ of $\mathcal{G}$ obtained by identifying each one of its nodes with the barycenter $b_{f(v^\star)}$ of the corresponding face $f(v^\star)$, and the arc connecting the nodes $v^\star$ and $w^\star$ with the segment $\overline{b_{f(v^\star)} b_{f(w^\star)}}$. Therefore, in the dual mesh $\mathcal{M}' := (B, G)$ each vertex $b_{f(v^\star)}$ corresponding to the face $f(v^\star) = (v_1, \dots, v_l)$ is computed as

$$b_{f(v^\star)} := \frac{1}{l} \sum_{i=1}^{l} p_{v_i}$$

and the connectivity G is completely defined by F. From the previous description it follows that each face of the dual mesh generally has a different number of vertices even if the input mesh is triangular, quadrilateral, etc. . Clearly, if $\mathcal{M}$ is a triangle mesh l is three.

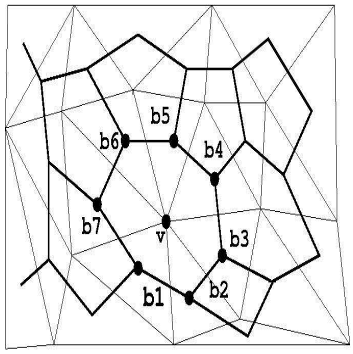

Figure 1. Triangle mesh and dual graph (marked line).

Finally, we note that the genus of the dual mesh is equal to that of the input mesh, thus preserving its topology. This simply follows observing that the Euler characteristic $\chi(\mathcal{M}) = n_V - n_E + n_F$ is the same of $\mathcal{M}^{'}$ being $n'_V = n_F$, $n'_E = n_E$, $n'_F = n_V$, where n_V, n_E, n_F and $n^{'}_V$, $n^{'}_E$, $n^{'}_F$ are the number of vertices, edges and faces of $\mathcal{M}$ and $\mathcal{M}^{'}$ respectively. Therefore, we can summarize this property as: *the genus of a polygonal mesh is invariant under the duality transformation.*

4. Combinatorial properties of triangle meshes

In the previous section we have derived the invariance of the genus of $\mathcal{M}$ under the duality transformation. We are now concerned with the analysis of the geometry of $\mathcal{M}$ and $\mathcal{M}^{'}$. The most general and strictly related questions which give a deeper understanding of the relationships and differences between $\mathcal{M}$ and $\mathcal{M}^{'}$ can be summarized as follows.

- Is it possible to locally characterize the 1-neighborhood structure of each vertex of $\mathcal{M}$?
- Is it possible to reconstruct the input mesh by using only the dual mesh? Which is the minimal number of information, if any, required for this purpose?

Answering these questions is not trivial and in the next section we take into consideration the case where $\mathcal{M}$ is a *2-manifold triangle mesh*; the analysis of the general problem is discussed in Section 4.3.

4.1. **1-neighborhood analysis.** In this section we are going to derive two basic combinatorial properties of the 1-neighborhood structure of each internal vertex v in $\mathcal{M}$. These relationships are used in the sequel for describing the linear reconstruction algorithm of $\mathcal{M}$ from $\mathcal{M}^{'}$ thus defining a complete topological and geometric identification between a mesh and its dual representation.

Theorem 1. *Let $\mathcal{M}$ be a 2-manifold triangle mesh with two adjacent vertices v and w, $VF(v) = (f_1, \dots, f_k)$ the faces incident in v, and b_i the barycenter of the face f_i, $\forall i = 1, \dots, k$ (see Figure 2). If v is an internal vertex, the following conditions hold:*

- *if k is even,*

$$\sum_{i=1}^{k}(-1)^i b_i = 0 \tag{1}$$

- *if k is odd,*

$$3\sum_{i=1}^{k}(-1)^{i+1} b_i = v + 2w \tag{2}$$

Proof. Considering $VV(v) = (v_1, \dots, v_k)$, with

$$a_1 := p_{v_1} = w,\ a_l := p_{v_l},\ l = 2, \dots, k$$

the idea is to express each vertex a_l as a linear combination of $\{b_i\}_{i=1}^{l-1}$, $2 \leq l \leq k$, v and w. For each triangle f_l, we have that

$$b_l = \frac{1}{3}(a_{l+1} + a_l + v) \Longleftrightarrow a_{l+1} = 3b_l - a_l - v.$$

Substituting in the last equality the expression of a_l in terms of b_{l-1}, a_{l-1}, v, and recursively applying this process we achieve that

$$a_{l+1} = \begin{cases} 3\sum_{i=1}^{l}(-1)^i b_i + a_1 & \text{if } l \text{ is even} \\ \\ 3\sum_{i=1}^{l}(-1)^{i+1} b_i - a_1 - v & \text{if } l \text{ is odd.} \end{cases}$$

The condition $a_{k+1} = a_1$ implies (1) if k is even, and (2) if k is odd. $\square$

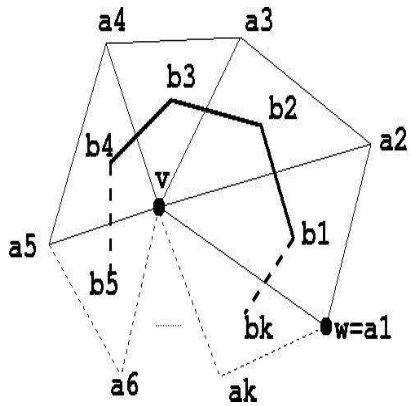

FIGURE 2. 1-neighborhood of the vertex v.

The interesting element in (1), (2) is that the coefficients which appear in the linear combination of the barycenters are constant and not related to their positions. Furthermore, if k is even the manifold structure on $\mathcal{M}$ ensures that $k \geq 4$; therefore, identifying b_i with the vector $(b_i - v)$ (2) gives their linear dependency relationship in the vector space $\mathbb{R}^3$ only using constant coefficients.

4.2. **Triangle mesh reconstruction through duality.** The first step of the reconstruction algorithm (see Figure 3) chooses two internal vertices v, w of an edge in $\mathcal{M}$ and associated to the neighborhoods

$$VV(v) = (v_1, \ldots, v_{n_1}), \quad VV(w) = (w_1, \ldots, w_{n_2}).$$

Selected the vertex v, each one of its incident triangles $VF(v) = (f_1, \ldots, f_{n_1})$, $n_1 \geq 3$, is represented by a vertex in the dual mesh $\mathcal{M}^{'}$ which is the barycenter of the related triangle in $\mathcal{M}$. Supposed to have calculated the vertices v, w and indicated with f one of the two triangles which have the segment $\overline{vw}$ as its edge, the third vertex u is evaluated as

$$u = 3b - v - w \tag{3}$$

where b is the barycenter of f.

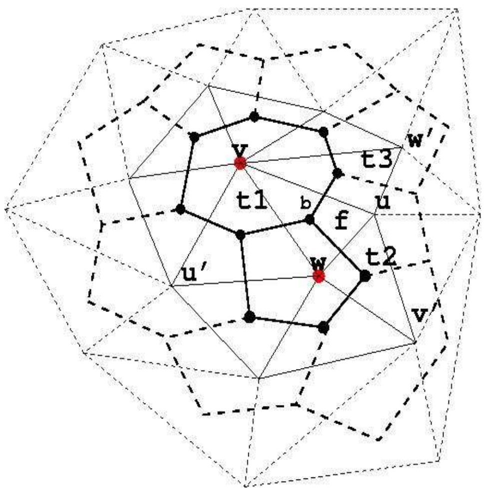

FIGURE 3. 1-neighborhoods of v and w used for the reconstruction of the mesh geometry.

After this calculation, the triangle f is marked as visited and its adjacent ones $(t_1, t_2, t_3) = FF(f)$ are considered. Using (3), the new vertices $u^{'}, v^{'}, w^{'}$ are calculated marking these triangles as visited. Growing from the visited faces by using their adjacent triangles, and recursively applying this criterion to the non-marked faces of $\mathcal{M}$ enables to reconstruct the geometry of the input mesh with exactly n_F steps.

It remains to describe the method for evaluating the two vertices v and w which have been used for reconstructing the input mesh geometry. Without loss of generality [2] we can suppose that n_1 and n_2 are odd; applying (2) to v and w leads to the symmetric linear system

$$\begin{cases} 3\sum_{i=1}^{n_1}(-1)^{i+1} b_i = 2w + v \\ \\ 3\sum_{i=1}^{n_2}(-1)^{i+1} b_i^{'} = 2v + w \end{cases}$$

[2]For instance, if n_1 is even we can split f_{n_1} into two new triangles; i.e. joining its vertex v with the middle point of the edge opposite to v in f_{n_1}.

where $VF(w) = (f_1^{'}, \ldots, f_{n_2}^{'})$ and $b_i^{'}$ is the barycenter of the face $f_i^{'}$. Because these relations are linearly independent, its unique solution is

$$\begin{cases} w = 2\alpha - \beta \\ v = 2\beta - \alpha \end{cases} \tag{4}$$

with $\alpha = \sum_{i=1}^{n_1}(-1)^{i+1}b_i$ and $\beta = \sum_{i=1}^{n_2}(-1)^{i+1}b_i^{'}$.

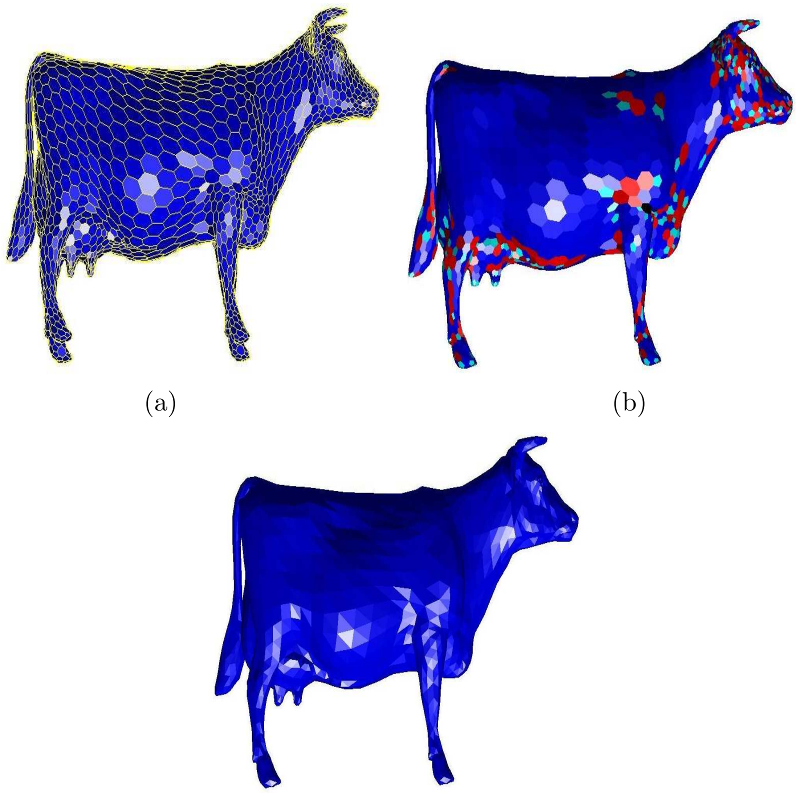

(a) (b)

(c)

FIGURE 4. (a) Input dual mesh with 5.804 vertices and 2.904 faces, (b) dual graph colored with respect to the number of vertices in each face (see Table 1), (c) reconstructed triangle mesh.

The relation (4) expresses these vertices as a linear combination of the barycenters of the triangles of their 1-neighborhoods; we also underline the symmetry in the expression of v and w with respect to α, β. The computational cost of the proposed algorithm is optimal because it only requires to visit all the triangles of the input mesh, and the expression (3) is computationally stable minimizing the numerical instability of the algorithm. Therefore, the transformation which maps $\mathcal{M}$ to $\mathcal{M}^{'}$ is linear in n_F as its inverse. An example of dual mesh and of the reconstruction process is given in Figure 4.

4.3. **Considerations on the primal-dual correspondence.** We present in this section several considerations on the primal-dual correspondence which is related to the dual Laplacian smoothing described in the following of the paper. The extension of the reconstruction

Table 1. Face coloring in the dual graph.

Color	Number of face vertices k
yellow	$1 \leq k < 2$
cyan	$2 \leq k < 6$
blue	$k = 6$
red	$7 \leq k < 10$
black	$k \geq 10$

process from the dual mesh of a q-mesh, $q \geq 4$, cannot be directly derived from the approach previously described. In fact, supposed that $(l-1)$ vertices $(p_{v_1}, \dots, p_{v_{l-1}})$ of a face $f = (v_1, \dots, v_l)$ in $\mathcal{M}$ have been calculated, the last vertex p_{v_l} is evaluated using the barycenter of f

$$b_f = \frac{1}{l}\sum_{i=1}^{l} p_{v_i}$$

as

$$p_{v_l} = l b_f - \sum_{i=1}^{l-1} p_{v_i};$$

however, this information is not sufficient for finding the position of all the vertices in the adjacent faces of f (see Figure 5).

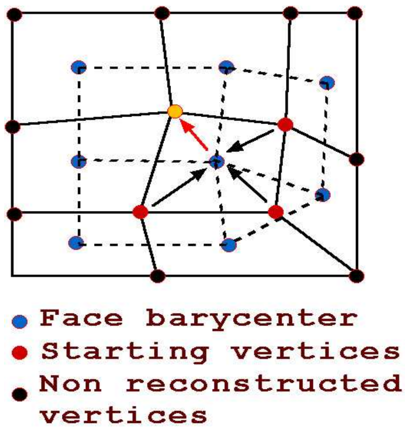

Figure 5. Quadrilateral mesh: dual representation (dotted line) and non-reconstructed geometry.

We answer questions given in Section 4 in a simple way as summarized by Theorem 2.

Theorem 2. *Given a 2-manifold triangle mesh $\mathcal{M}$ with or without boundary and with at least two internal vertices, the following conditions hold:*

- *$\mathcal{M}$ and its dual mesh $\mathcal{M}'$ are topologically equivalent, i.e. $\chi(\mathcal{M}) = \chi(\mathcal{M}')$;*
- *$\mathcal{M}$ and $\mathcal{M}'$ are geometrically equivalent, i.e. $\mathcal{M}$ (resp. $\mathcal{M}'$) is reconstructed in n_F steps (resp. n_V) from its dual representation $\mathcal{M}'$ (resp. $\mathcal{M}$);*
- *the vertices of $\mathcal{M}$ and $\mathcal{M}'$ satisfy conditions (1), (2) given in Theorem 1.*

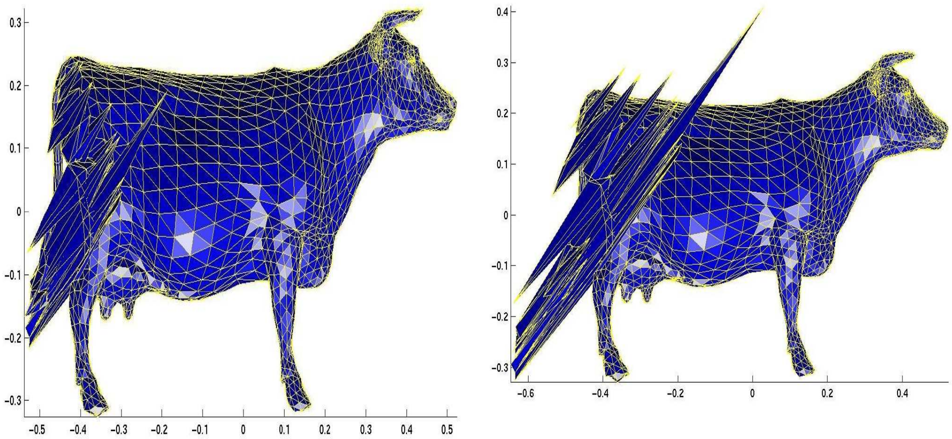

(a) (b)

FIGURE 6. Noise influence on the reconstruction process using: (a) noised vertices $\tilde{v}$, $\tilde{w}$ in $\mathcal{M}$, $e := 5.0{*}10^{-6}$, (b) a noised vertex in $\mathcal{M}'$, $e := 5.0{*}10^{-6}$.

In Theorem 2, it has been pointed out that the dual mesh is sufficient for identifying the input triangle mesh geometry and topology without storing additional information. We want to analyze the influence of the information in $\mathcal{M}'$ for the reconstruction process; equivalently, we study how the geometry of $\mathcal{M}$ is affected by changing the position of v and w. To this end, we add a noise e to each one of them considering the new points

$$\tilde{v} := v + e, \qquad \tilde{w} := w + e.$$

Denoted with $\mathcal{M}$ the triangle mesh reconstructed from $\mathcal{M}'$, v, w and with $\mathcal{M}_{noise}$ the one achieved with $\mathcal{M}'$, $\tilde{v}, \tilde{w}$, we want to estimate their deviation by using a norm for the error evaluation. The comparison of two triangle meshes with different geometry and connectivity has been studied in [4]. Because $\mathcal{M} := (P, F)$ and $\mathcal{M}_{noise} := (\tilde{P}, F)$ share the same topology, a simpler comparison between vertex positions and triangle normals is introduced using the following vectors:

$$d_v(\mathcal{M}, \mathcal{M}') := \left(\frac{\|p_i - \tilde{p}_i\|_2}{C_V} \right)_{i=1}^{n_V}, \; C_V := \max_{i=1,\ldots,n_V} \{\|p_i - \tilde{p}_i\|_2\}$$
$$d_n(\mathcal{M}, \mathcal{M}') := \left(\frac{\|n_i - \tilde{n}_i\|_2}{C_N} \right)_{i=1}^{n_F}, \; C_N := \max_{i=1,\ldots,n_F} \{\|n_i - \tilde{n}_i\|_2\}$$

with n_i and $\tilde{n}_i$ unit normals to the faces f_i and f_i'. For a better visualization, the increasing reorder of $d_v(\mathcal{M}, \mathcal{M}')$ and $d_n(\mathcal{M}, \mathcal{M}')$ is plotted without normalization (i.e. $C_V := C_N := 1$). As underlined in Figure 6(a), a small perturbation e creates a wrong reconstruction of the input triangle mesh showed in Figure 4(c). This phenomena is mainly due to the high correlation between vertices in $\mathcal{M}$ and $\mathcal{M}'$ resulting in an error propagation which grows in parallel with the visiting triangle process. This aspect is a consequence of the fact that each new vertex is calculated starting from those ones previously evaluated; indeed, after k steps (3) results affected by an error which is proportional to e^k. These considerations also apply if we add a noise to the vertices in $\mathcal{M}'$ as underlined Figure 6(b). Figure 7 shows all steps of the proposed framework.

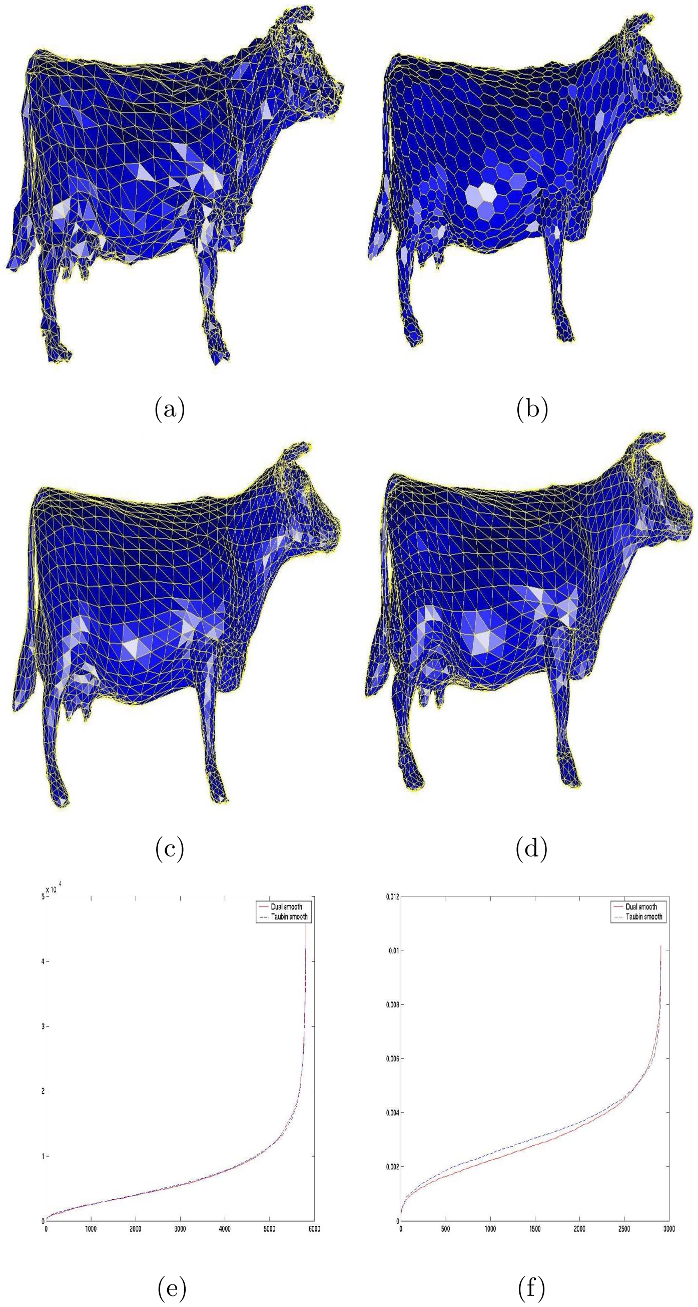

FIGURE 7. (a) Input data set: num. vertices 2.904, num. triangles 5.804, (b) Laplacian smoothing applied to the dual mesh $\lambda = 0.6$, $\mu = -0.5640$, $k = 10$, (c) average reconstruction, (d) Taubin's smoothing with previous λ, μ, k, (e) error evaluation on vertices, (f) error evaluation on normals.

We associate to a mesh three matrices which code in a compact form its topology. If $VF(v) = (f_1, \ldots, f_m)$ is the set of faces incident in a vertex v of $\mathcal{M}$, we construct the corresponding face-vertex matrix $I_{VF} \in M_{n_V,n_F}(\mathbb{R})$

$$I_{VF}(i,j) := \begin{cases} 1 & \text{if } f_j \in VF(v_i), \\ 0 & \text{else} \end{cases} \tag{5}$$

and its normalization

$$N_{VF}(i,j) := \begin{cases} 1/m_i & \text{if } f_j \in VF(v_i),\ \#VF(v_i) = m_i, \\ 0 & \text{else.} \end{cases}$$

In a similar way, we define the normalized vertex-vertex matrix $N_{VV} \in M_{n_V,n_V}(\mathbb{R})$ as

$$N_{VV}(i,j) := \begin{cases} 1/m_i & \text{if } v_j \in VV(v_i),\ \#VV(v_i) = m_i, \\ 0 & \text{else} \end{cases}$$

and the normalized vertex-face matrix $N_{FV} \in M_{n_F,n_V}(\mathbb{R})$

$$N_{FV}(i,j) := \begin{cases} 1/m_i & \text{if } v_j \in FV(f_i),\ \#FV(f_i) = m_i, \\ 0 & \text{else.} \end{cases}$$

The properties of their spectrum have important connections with the topological characteristics (e.g. number of connected components) of the input mesh [15] and with numerical properties of the Laplacian smoothing and re-sampling operator studied in [18, 17, 20]. Using these matrices, we want to settle the numerical approach to the reconstruction process from $\mathcal{M}$ to $\mathcal{M}^{'}$, which is expressed as

$$N_{FV}P = B, \tag{6}$$

that is, a linear system with n_V unknowns $(p_i)_{i=1}^{n_V}$ and n_F equations.

Because $n_F \approx 2n_V$, (6) is undetermined if $rank(N_{FV}) < n_V$, over-determined if $rank(N_{FV}) > n_V$ and it has a unique solution otherwise. In order to define a well-posed problem, (6) can be replaced by the *least-square problem* [9]

$$\|N_{FV}\bar{P}_i - B_i\|_2 = \min_{P_i}\{\|N_{FV}P_i - B_i\|_2\},$$

or equivalently $N_{FV}^T N_{FV}\bar{P}_i = N_{FV}^T B_i$, $i = 1, 2, 3$ where P_i and B_i is the i-th component of P and B respectively. This choice produces a family of triangle meshes $\{\tilde{P}\}$

$$\tilde{P}_i := \bar{P}_i + E_i, \qquad E_i \in ker(N_{FV}), \qquad i = 1, 2, 3$$

each one represents an approximated solution of (6), and the computational cost is $O(n_V^3)$. With respect to the primal-dual correspondence described in Section 4.2, this strategy faces-up to its expensive computational cost providing a family of approximated triangle meshes $(\tilde{P}, F)$ instead of the initial mesh $\mathcal{M}$.

5. Dual Laplacian smoothing

In the previous section we have focused our attention on the relationships between a triangle mesh $\mathcal{M}$ and its dual representation underlining their correlation. Here, we consider applications of the dual representation for smoothing noised data sets. The key observation is that, considering the 1-neighborhood structure related to each point, $\mathcal{M}$ has a little regularity while $\mathcal{M}^{'}$ can be considered with more simplicity because each of its vertices has three links if the related triangle of $\mathcal{M}$ is internal, and one/two if it belongs to the mesh boundary. This observation is the base in [13] for the compression of triangle meshes; furthermore, primal-dual correspondence is partially exploited in [21] for primal-dual subdivision schemes, and in [18] for the definition of dual re-sampling and non-shrinking smoothing operators. Firstly, we review Laplacian and Taubin's smoothing algorithms [18, 17, 20] which are strictly related to our approach, and we refer the reader to [2] for a complete description and comparison of mesh regularization methods.

- **Laplacian smoothing.** Each internal vertex p_v of the input mesh is updated using its 1-neighborhood structure $VV(v) := (v_1, \ldots, v_n)$ as described by the following procedure:
$$p_v^{(1)} := (1-\lambda)p_v + \frac{\lambda}{\sum_{i=1}^n w_i} \sum_{i=1}^n w_i p_{v_i}$$
where $\lambda \in [0,1]$ is a positive parameter controlling the smoothing process. The weights $(w_i)_{i=1}^n$ can be chosen in different ways even if the following ones are commonly used:
  - *constant weights*: $w_i = 1,\ i = 1, \ldots, n$, i.e.

(7)
$$p_v^{(1)} := (1-\lambda)p_v + \frac{\lambda}{n} \sum_{i=1}^n p_{v_i}.$$

  - *adaptive weights* [17]: w_i is proportional to the inverse of the distance between p_v and its neighbor p_{v_i}, i.e. $w_i := \|p_v - p_{v_i}\|_2^{-1}$. A general choice is given by $w_{ij} \geq 0$, $\sum_j w_{ij} = 1$ whose properties rely on the stochastic matrix theory [9, 19].

  We write (7) as
$$P^{(1)} = [(1-\lambda)I_{n_V} + \lambda N_{VV}]P = f_\lambda(L)P$$
where I_{n_V} is the identity matrix of order n_V, $f_\lambda(t) = (1-\lambda t)$, $L := I_{n_V} - N_{VV}$ and
$$P = \begin{pmatrix} p_1 \\ \vdots \\ p_{n_V} \end{pmatrix} \in M_{n_V,3}(\mathbb{R}).$$
The Laplacian smoothing reduces all non-zero frequencies of the signal corresponding to the mesh and tends to shrink its geometry. To partially solve this drawback, in [7] each smoothing iteration is combined with a mesh volume-restoring and re-scaling step.
- **Taubin's smoothing.** The solution to shrinkage proposed in [17] is based on the alternation of two scale factors of opposite signs λ, μ in the Laplacian smoothing, i.e.
$$P_{Taubin}^{(1)} := f_\lambda(L) f_\mu(L) P$$
where $-\mu > \lambda > 0$. Using this filter enables to suppress high frequencies while preserving the low ones. Good results are achieved by choosing the input parameters which satisfy the condition
$$\frac{1}{\lambda} + \frac{1}{\mu} = 0.1.$$
The application of k iteration steps gives
$$P_{Taubin}^{(k)} = f_{\lambda,\mu}^{(k)}(L)P$$
with $f_{\lambda,\mu}^{(k)}(t) := [f_\lambda(t) f_\mu(t)]^k$.

5.1. **Dual approach to triangle mesh smoothing.** Considered a noised mesh $\mathcal{M}_{noise} := (P, F)$, the idea is to apply the Laplacian smoothing and its extensions proposed in [18, 17, 20] to the dual mesh $\mathcal{M}^{'}_{noise} := (B, G)$ which is affected by noise as well as $\mathcal{M}_{noise}$. The merit of using the dual mesh instead of the input one is mainly due to the following considerations. Firstly, the normalized vertex-vertex matrix N_{FF} of $\mathcal{M}^{'}_{noise}$, which will be used for the smoothing process, has at most three non zero elements in each row. This implies the optimization of storage and computational requirements which grow with the complexity of the input mesh in terms of the number of vertices. Furthermore, the construction of the incident matrix of $\mathcal{M}^{'}_{noise}$ is simply achieved with the constant relation FF applied to $\mathcal{M}$. Secondly, the dual smoothing considers at each vertex of $\mathcal{M}$ a different topology for the regularization with respect to the 1-neighborhood structure used for the (primal) Laplacian smoothing (see Figure 8).

Denoted with with $L^{'}$ the Laplacian matrix of $\mathcal{M}^{'}_{noise}$, and with $\mathcal{M}^{'}_{smooth}$ the smoothed dual mesh, the last step reconstructs the regularized mesh $\mathcal{M}_{smooth}$. Because of the vertices of $\mathcal{M}^{'}_{smooth}$ do not satisfy (1), (2), the considerations about the high correlation between $\mathcal{M}^{'}_{smooth}$ and $\mathcal{M}_{smooth}$ (see Section 4.3) highlight the impossibility of reconstructing $\mathcal{M}_{smooth}$ by using the primal-dual correspondence previously described. The solution to this problem is achieved by defining the new vertices of $\mathcal{M}_{smooth} := (P_{smooth}, F)$ as the barycenters of the faces in $\mathcal{M}^{'}_{smooth}$ which are exactly n_V. This process can be summarized as

$$P^{(k)}_{smooth} = N_{VF}\,\underbrace{f^{(k)}_{\lambda,\mu}(L^{'})B}_{\text{Dual smooth}} = N_{VF} f^{(k)}_{\lambda,\mu}(L^{'}) N_{FV} P \qquad (8)$$

with $L^{'} := I_{n_F} - N_{FF}$. The previous relation expresses the regularized mesh geometry only using the information on $\mathcal{M}_{noise}$.

We now compare (8) with the mesh achieved by applying the Taubin's smoothing using the same number of iterations k, and parameters $\bar{\lambda}$, $\bar{\mu}$

$$P^{(k)}_{Taubin} = f^{(k)}_{\bar{\lambda},\bar{\mu}}(L)P.$$

From the previous relation, it follows that [3]

$$\frac{\|P^{(k)}_{smooth} - P^{(k)}_{Taubin}\|_2}{\|P\|_2} \leq \|N_{FV}\|_2 \|N_{VF}\|_2 g^k(\lambda,\mu) + g^k(\bar{\lambda},\bar{\mu})$$

with $g(x,y) := \frac{(x-y)^2}{-4xy}$. Because $|\lambda| < 1$, $|\mu| < 1$ (resp. $|\bar{\lambda}| < 1$, $|\bar{\mu}| < 1$), we have $|g(\lambda,\mu)| < 1$ (resp. $|g(\bar{\lambda},\bar{\mu})| < 1$) thus guaranteeing that

$$\lim_{k\to+\infty} \|P^{(k)}_{smooth} - P^{(k)}_{Taubin}\|_2 = 0,$$

i.e. *the asymptotic behavior of $P^{(k)}_{smooth}$ resembles that of $P^{(k)}_{Taubin}$ and its computational cost is linear in the number of vertices n_V.* All previous considerations also apply if we consider adaptive weights instead of constant ones. Finally, we observe that we have not applied the least square approach (6) for reconstructing $\mathcal{M}$ from $\mathcal{M}^{'}$ because it is computationally expensive and without evident benefits with respect to the previous choice. Other examples of the proposed approach are given in Figure 9, 10.

[3] The inverted parabola $f_{\lambda,\mu}(t) := (1-\lambda t)(1-\mu t)$ has its minimum at $\bar{t} := \frac{1}{2}(\frac{1}{\lambda} + \frac{1}{\mu}) \in (0,1)$ and $f_{\lambda,\mu}(\bar{t}) = \frac{(\lambda-\mu)^2}{-4\lambda\mu}$.

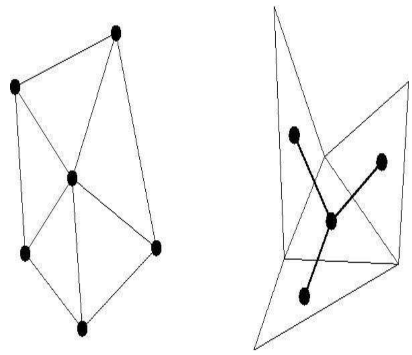

Figure 8. Topological masks used for the primal and dual Laplacian smoothing.

6. Conclusions and future work

The first goal of the paper is the definition of a homeomorphism between a 2-manifold triangle mesh and its dual representation with optimal (i.e. linear) computational cost and numerical stability avoiding the least-square formulation whose solution requires $O(n_V^3)$ flops and it only achieves an approximated reconstruction of the input mesh. We have also derived two combinatorial properties (1), (2) which highlight the redundancy of the geometry stored in a triangle mesh [12], and a deeper analysis of these properties have currently been studying. Finally, the duality analysis has been exploited for defining the dual Laplacian smoothing in order to settle a linear regularization method based on the face-face topological mask instead of the vertex-vertex one used by the Taubin's signal processing framework. This new approach has been compared with previous work highlighting its validity and optimality.

Acknowledgements This work has been partially supported by the National Project "MACROGeo: Metodi Algoritmici e Computazionali per la Rappresentazione di Oggetti Geometrici", FIRB grant. Thanks are given to the Computer Graphics Group of IMATI-GE, and to B. Falcidieno.

References

[1] F. Aurenhammer. Voronoi diagrams: A survey of a fundamental geometric data structure. *ACM Computing Surveys*, 23(3):345–405, Sept. 1991.

[2] A. Belyaev and Y. Ohtake. A comparison of mesh smoothing methods. *To appear in Israel-Korea Bi-National Conference on Geometric Modeling and Computer Graphics*, Tel-Aviv, Fabr. 12-14, 2003.

[3] M. W. Bern and D. Eppstein. Mesh generation and optimal triangulation. In F. K. Hwang and D.-Z. Du, editors, *Computing in Euclidean Geometry*, pages 23–90. World Scientific, 1992.

[4] P. Cignoni, C. Rocchini, and R. Scopigno. Metro: Measuring error on simplified surfaces. *Computer Graphics Forum*, 17(2):167–174, June 1998.

[5] M. de Berg, M. van Kreveld, M. Overmars, and O. Schwarzkopf. *Computational Geometry Algorithms and Applications.* Springer-Verlag, Berlin Heidelberg, 1997.

[6] L. DeFloriani and P. Magillo. Multiresolution mesh representation: Models and data structures. In *Tutorials on Multiresolution in Geometric Modeling*, pages 363–417, Munich, 2002. Springer-Verlag.

[7] M. Desbrun, M. Meyer, P. Schröder, and A. H. Barr. Implicit fairing of irregular meshes using diffusion and curvature flow. In A. Rockwood, editor, *Siggraph 1999*, Annual Conference Series, pages 317–324, Los Angeles, 1999. ACM Siggraph, Addison Wesley Longman.

[8] H. Edelsbrunner. *Algorithms in Combinatorial Geometry*, volume 10 of *EATCS Monographs on Theoretical Computer Science.* Springer-Verlag, Nov. 1987.

[9] G. Golub and G. VanLoan. *Matrix Computations.* John Hopkins University Press, 2nd. edition, 1989.

[10] L. J. Guibas and J. Stolfi. Primitives for the manipulation of general subdivisions and the computation of Voronoi diagrams. In *Proceedings of the Fifteenth Annual ACM Symposium on Theory of Computing*, pages 221–234, Boston, Massachusetts, 25–27 Apr. 1983.

[11] H. Hoppe, T. DeRose, T. Duchamp, J. McDonald, and W. Stuetzle. Surface reconstruction from unorganized points. *Computer Graphics*, 26(2):71–78, July 1992.

[12] M. Isenburg, S. Gumhold, and C. Gotsman. Connectivity shapes. In *Visualization'01 Conference Proceedings*, pages 135–142, 2001.

[13] J. Li and C. Kuo. A dual graph approach to 3D triangular mesh compression. In *IEEE 1998 International Conference on Image Processing, Chicago, Oct. 4-7, 1998.*, pages 891–894.

[14] M. Mäntylä. *An Introduction to Solid Modeling*. Computer Science Press, Rockville, MD, 1987.

[15] B. Mohar. The laplacian spectrum of graphs. *Graph Theory, Combinatorics and Applications.*, pages 871–898, 1991.

[16] F. P. Preparata and M. Shamos. *Computational Geometry*. Springer-Verlag, New York, 1985, 1985.

[17] G. Taubin. A signal processing approach to fair surface design. In R. Cook, editor, *SIGGRAPH 95 Conference Proceedings*, Annual Conference Series, pages 351–358. ACM SIGGRAPH, Addison Wesley, Aug. 1995. held in Los Angeles, California, 06-11 August 1995.

[18] G. Taubin. Dual mesh resampling. In *Proceedings of Pacific Graphics 2001*, pages 180–188, 2001. Tokyo, Japan, October 2001.

[19] G. Taubin. Geometric signal processing on polygonal meshes. In *Eurographics'2000, State of the Art Report*, August 2000.

[20] G. Taubin, T. Zhang, and G. Golub. Optimal surface smoothing as filter design. In B. Buxton and R. Cipolla, editors, *Computer vision, ECCV '96: 4th European Conference on Computer Vision, Cambridge, UK, April 15–18, 1996: proceedings*, volume 1064–1065 of *Lecture notes in computer science*, pages 283–292 (vol. 1). Springer-Verlag, 1996.

[21] D. Zorin and P. Schröder. A unified framework for primal/dual quadrilateral subdivision schemes. *Computer Aided Geometric Design*, Special issue on Subdivision Surfaces, 18, 2001., 2001.

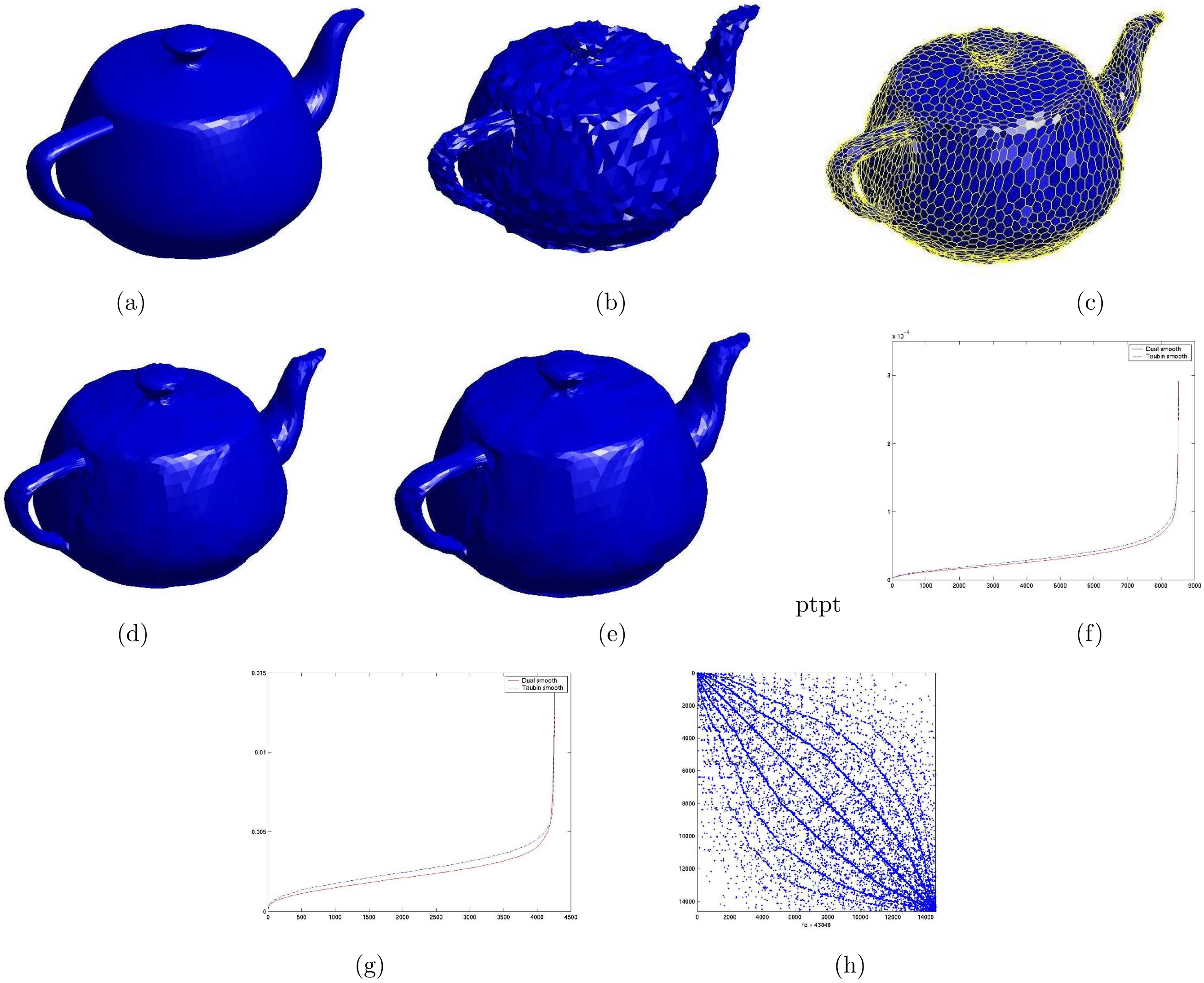

Figure 9. (a) Input data set: num. vertices 7.308, num. triangles 14.616, (b) noised data set with normal error, (c) Laplacian smoothing applied to the dual mesh $\lambda = 0.6$, $\mu = -0.5640$, $k = 20$, (d) average reconstruction, (e) Taubin's smoothing with previous λ, μ, k, (f) error evaluation on vertices, (g) error evaluation on normals, (h) Laplacian matrix sparsity.

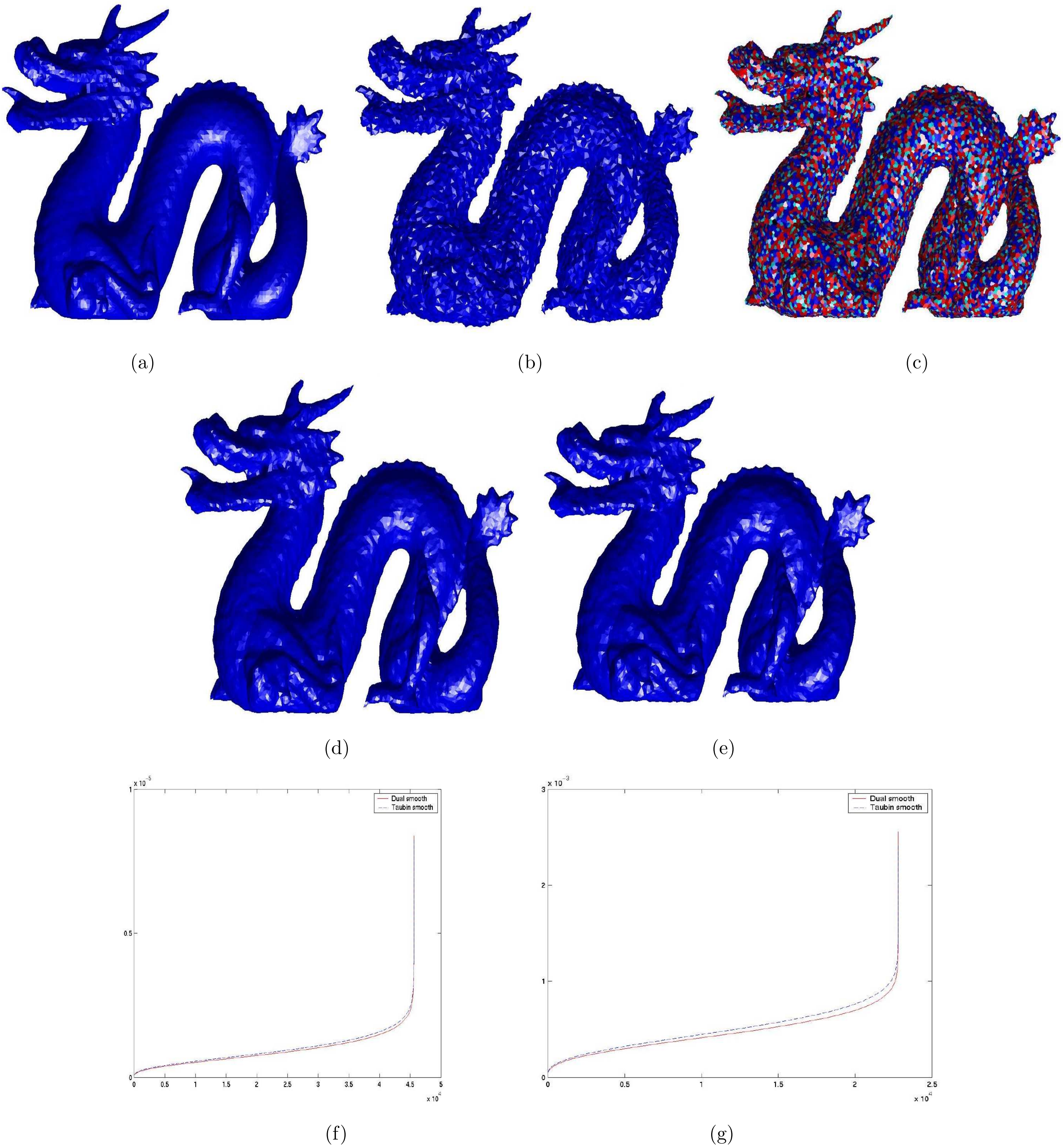

FIGURE 10. (a) Input data set: num. vertices 22.813, num. triangles 45.626, (b) noised data set with normal error, (c) Laplacian smoothing applied to the dual mesh $\lambda = 0.6$, $\mu = -0.5640$, $k = 10$, (d) average reconstruction, (e) Taubin's smoothing with previous λ, μ, k, (f) error evaluation on vertices, (g) error evaluation on normals.